

Characterizing Genuine Multilevel Entanglement

Tristan Kraft,^{1,*} Christina Ritz,^{1,*} Nicolas Brunner,² Marcus Huber,³ and Otfried Gühne¹

¹Naturwissenschaftlich-Technische Fakultät, Universität Siegen, Walter-Flex-Straße 3, 57068 Siegen, Germany

²Département de Physique Théorique, Université de Genève, 1211 Genève, Switzerland

³Institute for Quantum Optics and Quantum Information,

Austrian Academy of Sciences, A-1090 Vienna, Austria

(Dated: 9th February 2018)

Entanglement of high-dimensional quantum systems has become increasingly important for quantum communication and experimental tests of nonlocality. However, many effects of high-dimensional entanglement can be simulated by using multiple copies of low-dimensional systems. We present a general theory to characterize those high-dimensional quantum states for which the correlations cannot simply be simulated by low-dimensional systems. Our approach leads to general criteria for detecting multilevel entanglement in multiparticle quantum states, which can be used to verify these phenomena experimentally.

PACS numbers: 03.65.Ta, 03.65.Ud

Introduction.— Entangled quantum systems are now routinely prepared and manipulated in labs all around the world, using all sorts of physical platforms. In particular, there has been tremendous progress for creating high-dimensional entangled systems, which can in principle contain a very large amount of entanglement [1–3]. This makes such systems interesting from the perspective of information processing, as they can enhance certain protocols in particular in quantum communications [4, 5]. At first sight, the tools of entanglement theory can readily be applied to experiments generating high-dimensional entangled states. After a closer look, however, one realizes that this is not the case in general. Let us illustrate our argument via a simple example.

Imagine an experimentalist who wants to demonstrate his ability to entangle two high-dimensional quantum systems. He decides to prepare the optimal resource state, the maximally entangled state, in increasingly large dimensions. First, he successfully entangles two qubits in the state $|\psi_2\rangle = (|00\rangle + |11\rangle)/\sqrt{2}$ and two qutrits in the state $|\psi_3\rangle = (|00\rangle + |11\rangle + |22\rangle)/\sqrt{3}$. While preparing the two ququart maximally entangled state $|\psi_4\rangle = (|00\rangle + |11\rangle + |22\rangle + |33\rangle)/2$ he realizes that he could also prepare the two-qubit Bell state $|\psi_2\rangle$ twice, see Fig. 1(a). Clearly, the two copies are equivalent to the maximally entangled state of two ququarts when identifying $|00\rangle_{A_1 A_2} \mapsto |0\rangle_A$, $|01\rangle_{A_1 A_2} \mapsto |1\rangle_A$, $|10\rangle_{A_1 A_2} \mapsto |2\rangle_A$, and $|11\rangle_{A_1 A_2} \mapsto |3\rangle_A$. Furthermore, using the source n times, the experimentalist prepares the state $|\psi_2\rangle^{\otimes n}$, which is equivalent to a maximally entangled state in dimension $2^n \times 2^n$. The experimentalist is thus enthusiastic, as he now has access to essentially any entangled state with an entanglement cost of at most n ebits. In particular this should allow him to implement enhanced quantum information protocols based on high-dimensional entangled states, which are proven to boost the performance of certain protocols.

Clearly, the view of the experimentalist is too

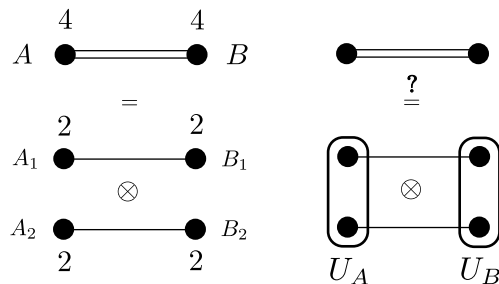


Figure 1: Left: The four-dimensional maximally entangled state $|\psi_4\rangle$ shared by the parties A and B directly decomposes in two entangled pairs of qubits shared by $A_1 B_1$ and $A_2 B_2$. Right: More generally, we ask whether a high-dimensional entangled state can be decomposed into pairs of entangled systems of smaller dimension, up to some local unitary operations. We show that this is not always possible and characterize those states carrying genuine multilevel entanglement.

simplistic and key aspects have been put under the carpet. In order to use the full potential of the state, and thus really claim to have access to high-dimensional entanglement, the experimentalist should be able to perform arbitrary local measurements, including joint measurements between the two subspaces (e.g., photons), which can be non-trivial to implement in certain experimental setups. Ideally, the experimentalist should be able to implement arbitrary local transformations on the local four-dimensional space.

If one focuses on the generated state, however, the known methods of entanglement verification support the naive view of the experimentalist. For instance, there are tools to certify the Schmidt rank of the state [6, 7], but these do not distinguish between many copies of a Bell state and a genuine high-dimensional state. Bell inequalities have been proposed as dimension witnesses for quantum systems [8], but recently it has turned out that these do not recognize the key feature, as independent

measurements on two Bell pairs can mimic the statistics of a high-dimensional system [9, 10]. So they just characterize the Schmidt rank in a device-independent manner.

In this work, we characterize the high-dimensional quantum states which give rise to correlations that can not be simulated many copies of small-dimensional systems. This leads to the notion of genuine multilevel entanglement and we show how this can be created and certified. Then we extend this idea to the multiparticle case. Our results imply that many of the prominent entangled states in high dimensions can directly be simulated with small-dimensional systems.

The scenario.— First we consider four-level systems, also called ququarts. A general two-qu quart entangled state can be written in the Schmidt decomposition as

$$|\psi\rangle = s_0|00\rangle_{AB} + s_1|11\rangle_{AB} + s_2|22\rangle_{AB} + s_3|33\rangle_{AB}, \quad (1)$$

where we assume here and in the following the Schmidt coefficients to be ordered, i.e., $s_0 \geq s_1 \geq s_2 \geq s_3 \geq 0$ and $\sum_i s_i^2 = 1$. One can replace each qu quart with two qubits, so the total state may also be considered as a four-qubit state. The question we ask is whether it is possible to reproduce any correlations in the two-qu quart state by preparing two entangled pairs of qubits only (see Fig. 1).

A first approach is to replace on Alice's side $|0\rangle \mapsto |00\rangle$, $|1\rangle \mapsto |01\rangle$, $|2\rangle \mapsto |10\rangle$, and $|3\rangle \mapsto |11\rangle$ and similarly for Bob. Note that this is, so far, not guaranteed to be the optimal assignment of basis states on two qubits to the basis states $\{|0\rangle, |1\rangle, |2\rangle, |3\rangle\}$. This replacement leaves us with the four-qubit state

$$|\psi\rangle = s_0|00\rangle_{A_1B_1}|00\rangle_{A_2B_2} + s_1|00\rangle_{A_1B_1}|11\rangle_{A_2B_2} + s_2|11\rangle_{A_1B_1}|00\rangle_{A_2B_2} + s_3|11\rangle_{A_1B_1}|11\rangle_{A_2B_2}. \quad (2)$$

Now we ask under which conditions this state can be decomposed as

$$|\varphi\rangle = (\alpha_0|00\rangle_{A_1B_1} + \alpha_1|11\rangle_{A_1B_1}) \otimes (\beta_0|00\rangle_{A_2B_2} + \beta_1|11\rangle_{A_2B_2}). \quad (3)$$

For the Schmidt coefficients it must hold that $s_0 = \alpha_0\beta_0$, $s_1 = \alpha_0\beta_1$, $s_2 = \alpha_1\beta_0$ and $s_3 = \alpha_1\beta_1$. If $|\psi\rangle$ can be written in this form, we call $|\psi\rangle$ decomposable and otherwise genuinely four-level entangled. An interesting example is the maximally entangled state of two ququarts, $|\psi_4\rangle = (|00\rangle_{AB} + |11\rangle_{AB} + |22\rangle_{AB} + |33\rangle_{AB})/2$. Here $s_i = 1/2$ and for $\alpha_0 = \alpha_1 = \beta_0 = \beta_1 = 1/\sqrt{2}$ we have $|\psi\rangle = |\varphi\rangle$. Thus the maximally entangled state is decomposable, its correlations are reproducible by two pairs of entangled qubits, and the state is not sufficient to certify genuine four-level entanglement.

In order to decide decomposability for a general $|\psi\rangle$ we compute the maximal overlap between $|\psi\rangle$ and all decomposable states $|\varphi\rangle$:

$$\begin{aligned} \max_{|\varphi\rangle} |\langle\psi|\varphi\rangle| &= \max_{\alpha_i, \beta_i} \{s_0\alpha_0\beta_0 + s_1\alpha_0\beta_1 + s_2\alpha_1\beta_0 + s_3\alpha_1\beta_1\} \\ &= \max_{\alpha, \beta} \langle\beta|S|\alpha\rangle = \max \text{singval}(S), \end{aligned} \quad (4)$$

where $|\alpha\rangle = (\alpha_0, \alpha_1)^T$, $|\beta\rangle = (\beta_0, \beta_1)^T$, and

$$S = \begin{bmatrix} s_0 & s_1 \\ s_2 & s_3 \end{bmatrix}, \quad (5)$$

and $\text{singval}(S)$ denotes the singular values.

Note that up to now, we have not determined the optimal choice for the basis assignment, that is, we used the simple assignment $|0\rangle \mapsto |00\rangle$ etc. introduced above. The optimal assignment can be determined by optimizing over local unitaries on the ququarts. In Appendix A [11] we show that the maximal singular value is obtained if the states $|\psi\rangle$ and $|\varphi\rangle$ have the same Schmidt basis and the remaining freedom encompasses permutations in the assignment of basis elements. As it turns out, the basis choice from the beginning is optimal and we have:

Observation 1. *The two-qu quart state $|\psi\rangle$ is decomposable if and only if $\max \text{singval}(S) = 1$. This is equivalent to $\det(S) = 0$. The proof is given in Appendix A [11].*

The extension of decomposability to mixed states is straightforward. We define a mixed state to be decomposable, if it can be written as $\varrho = \sum_i p_i |\psi_i\rangle\langle\psi_i|$ where the $|\psi_i\rangle$ are decomposable, and genuine four-level entangled otherwise. The set of decomposable states \mathcal{D} is convex by definition. This allows to construct witnesses for four-level entanglement. Recall that an operator \mathcal{W} is called an entanglement witness, iff $\text{tr}(\sigma\mathcal{W}) \geq 0$ for all separable states σ and $\text{tr}(\varrho\mathcal{W}) < 0$ for at least one entangled state ϱ [12]. A special type of witnesses are the projector-based witnesses which are of the form $\mathcal{W} = \alpha\mathbb{1} - |\xi\rangle\langle\xi|$, where α is the maximal squared overlap between $|\xi\rangle$ and the decomposable states [13]. In order to detect as many states as possible, we chose $|\xi\rangle$ to be the state with the largest distance to \mathcal{D} , meaning that α is as small as possible. The state $|\xi\rangle$ can be determined by minimizing the maximal singular value of S in Eq. (4) which is, according to Observation 1, a function of squared determinant. Thus we distinguish between positive and negative values of the determinant, giving two interesting states $|\xi_i\rangle$, see Appendix B [11] for details:

Observation 2. *The following two states locally maximize the distance to the decomposable states: For $\det(S) < 0$ the Schmidt-rank three state*

$$|\xi_1\rangle = \frac{1}{\sqrt{3}}(|00\rangle + |11\rangle + |22\rangle) \quad (6)$$

has the largest distance with $\alpha = [(3 + \sqrt{5})/6]^{1/2} \simeq 0.934$ to the set of decomposable states. For $\det(S) > 0$ the Schmidt-rank four state

$$|\xi_2\rangle = \sqrt{\frac{3}{4}}|00\rangle + \frac{1}{2\sqrt{3}}(|11\rangle + |22\rangle + |33\rangle) \quad (7)$$

maximizes the distance with a value of $\alpha = [(3 + 2\sqrt{2})/6]^{1/2} \simeq 0.986$ to the set of decomposable states.

General theory for bipartite systems.— Let us start by considering only decompositions into two lower-dimensional states. In this case the results from the previous section still hold, only the matrix S increases according to the dimensions of the subsystems. This leaves us with the problem that the maximal singular value depends on the encoding, which defines the arrangement of Schmidt coefficients in the matrix S .

As an example we consider the embedding of the rank-four state from Eq. (1) in a 6×6 dimensional system, that is, each party has a qubit and a qutrit. Using the encoding $|0\rangle \mapsto |00\rangle, |1\rangle \mapsto |01\rangle, |2\rangle \mapsto |02\rangle, |3\rangle \mapsto |10\rangle, |4\rangle \mapsto |11\rangle, |5\rangle \mapsto |12\rangle$ we obtain the matrix S_1 whereas using $|0\rangle \mapsto |00\rangle, |1\rangle \mapsto |01\rangle, |2\rangle \mapsto |10\rangle, |3\rangle \mapsto |11\rangle, |4\rangle \mapsto |02\rangle, |5\rangle \mapsto |12\rangle$ we obtain a different matrix S_2 . The matrices are given by

$$S_1 = \begin{bmatrix} s_0 & s_1 & s_2 \\ s_3 & s_4 & s_5 \end{bmatrix}, \quad S_2 = \begin{bmatrix} s_0 & s_1 & s_4 \\ s_2 & s_3 & s_5 \end{bmatrix} \quad (8)$$

and can lead to different singular values. For instance, if we embed the two-ququart state $|\psi_4\rangle$ in this configuration, i.e., $s_0 = s_1 = s_2 = s_3 = 1/2$ and $s_4 = s_5 = 0$, we find that $\max \text{singval}(S_1) \neq 1$, whereas $\max \text{singval}(S_2) = 1$. Consequently, when deciding decomposability, it is crucial to optimize over all possible permutations of entries in S . As the number of permutations grows super-exponentially, it is in general hard to compute this for increasing dimensions.

Nevertheless, the complexity can be reduced, as we have to consider only those permutations which lead to different maximal singular values. In Appendix C [11] we discuss this simplification which leads to the theory of Young tableaux [14]. It turns out that for a decomposition into $d = d_1 \times d_2$ there are at most

$$\mathcal{N} = \frac{(d_1 \times d_2)!}{\prod_{i=1}^{d_1} \prod_{j=1}^{d_2} (i+j-1)} \quad (9)$$

different matrices that could lead to different singular values. Examples can be found in Appendix B [11].

Furthermore, if one is only interested in decomposability, it suffices to check whether there exists an arrangement such that S has rank one. The number of possible arrangements reduces to at most

$$\mathcal{N}' = \frac{(d_1 + d_2 - 2)!}{(d_1 - 1)! \times (d_2 - 1)!}. \quad (10)$$

It should be noted that an equivalent problem and solution has been considered in quantum thermodynamics, where one may ask whether the correlations in a bipartite system can drop to zero under global unitaries [15].

To complete the discussion, one may also take into account a decomposition of the system into more than two lower-dimensional subsystems. In this case, the matrix S becomes a tensor and thus deriving an analytical expression, equivalent to the singular value decomposition,

is difficult. However, one can construct an iterative algorithm to calculate the maximal overlap between the original state and a given set of decomposable states as follows: The total maximization can be split into a maximization over states and local unitaries. If all but one of these objects are fixed, the remaining one can be carried out analytically. This leads to a fast iteration, see Appendix E [11] for a detailed discussion.

Multiparticle systems.— We call an N -partite pure state $|\psi\rangle$ in $(\mathbb{C}^D)^{\otimes N}$ fully decomposable iff there exist N -partite states $|\varphi\rangle, |\varphi'\rangle$ of dimension d, d' such that:

$$|\psi\rangle = U_1 \otimes \dots \otimes U_N |\varphi\rangle \otimes |\varphi'\rangle, \quad (11)$$

for some $d \times d' = D$. Here, the U_i denote the unitaries each party applies to their local subsystems. This definition is in analogy to full separability in entanglement theory [13]. A state that is not fully decomposable is multipartite multilevel entangled (MME).

If a state is non-decomposable according to Eq. (11), there might exist partitions under which such states are decomposable. For instance, a state may be decomposable, if the unitary on the first two particles is allowed to be nonlocal, i.e., we may set $U_1 \otimes U_2 \mapsto U_{12}^{\text{nl}}$. More generally, there may be a bipartition of the N particles for which the state is decomposable.

Observation 3. *Consider an N -particle state $|\psi\rangle$. If there exists a bipartition $M|M'$ of the N particles for which the state is decomposable, the state is called bidecomposable. Otherwise the state is genuinely multipartite multilevel entangled (GMME). Verifying GMME for pure states can be done by applying the methods for bipartite systems to all bipartitions.*

To show that a pure multiparticle state is not fully decomposable is, however, not straightforward, as there is in general no Schmidt decomposition for systems consisting of more than two parties [16]. Nevertheless, the iterative algorithm mentioned above can again be utilized. Note that within the optimally decomposed state, the largest block that cannot be decomposed any further identifies the minimal number of parties and dimensions needed to reproduce the correlations in the original state. Also, the definitions above can be readily generalized to mixed states by considering convex combinations. In the following sections, we discuss examples which are relevant for current experiments.

Example 1: Generalized GHZ states.— Motivated by our result from the bipartite case that the maximally entangled state is decomposable, we start with studying Greenberger-Horne-Zeilinger (GHZ) states, $|GHZ^{(D)}\rangle = \frac{1}{\sqrt{D}}(|0 \dots 0\rangle + |1 \dots 1\rangle + \dots + |(D-1) \dots (D-1)\rangle)$ for N particles with local dimension D .

First, we observe that the GHZ state is fully decomposable. In fact, it is decomposable with respect to the finest factorization of the local dimension D , given by the

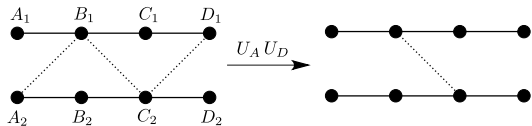


Figure 2: Examples of weighted graph states. Left: The four-ququart chain-graph state from Eq. (14) can be encoded into a weighted graph state of eight qubits, see Eq. (16). Right: After application of the unitaries $U_{A_1 A_2}$ and $U_{D_2 D_1}$ the state exhibits decomposability with respect to the bipartitions $A|BCD$, $D|ABC$ and $AD|BC$ [see Eq. (17)] and thus the original ququart state is bidecomposable and not GMME.

prime decomposition $D = \prod_{j=1}^k d_j$ of D , as we can write:

$$|GHZ^{(D)}\rangle \stackrel{enc.}{=} \bigotimes_{j=1}^k |GHZ^{(d_j)}\rangle, \quad (12)$$

where $|\varphi_j\rangle$ represents the N -partite state of the subsystem with dimension d_j .

The proof is straightforward. We just replace each level $|i\rangle$ (with $i \in [0, D-1]$) of the original state with its respective encoding into the lower levels $|i_1, \dots, i_k\rangle$ where each i_j has dimension d_j and as such values $\in [0, d_j-1]$ for all j . The ordering of the encoding is chosen such that the value within the respective number system is increasing, that is it corresponds to a binary encoding for qubits ($d_j = 2$), ternary for qutrits ($d_j = 3$), and similarly for higher dimensions. This leads to $|0\rangle \mapsto |0 \dots 0\rangle, \dots, |D-1\rangle \mapsto |\bigotimes_j (d_j - 1), \dots, \bigotimes_j (d_j - 1)\rangle$. Following this encoding process, a reordering, that is $(A_1 \dots A_n, B_1 \dots B_n, \dots) \mapsto (A_1 B_1 \dots, \dots, A_n B_n \dots)$, directly reveals the tensor structure of the encoded state with respect to every factor d_j . In Appendix D [11] we give the calculation for a six-dimensional GHZ state. Furthermore we show there that the absolutely maximally entangled state of six qubits represents a decomposable three-ququart state in the GHZ class.

So all the correlations of a GHZ state in high dimensions, although having a high Schmidt-rank for the bipartitions, can be simulated by low-dimensional systems. This is distinct from other approaches, such as the Schmidt number vectors from Ref. [17] or the criterion in Ref. [18], where the GHZ state was used to detect higher-order entanglement. For completeness, a proof of the LU-equivalence between GHZ- and the star-type graph states from Ref. [18] is given in Appendix D [11].

Example 2. Graph states. — A D -dimensional weighted graph state can be written as [19, 20]

$$|G\rangle = \prod_{\{ij\} \in E} Z_{\{ij\}}^\alpha |+\rangle^{\otimes V}, \quad (13)$$

where V denotes the set of vertices, E the set of edges connecting two vertices i and j and $|+\rangle^{\otimes V}$ is given by $|+\rangle^{\otimes V} \propto |0\rangle + |1\rangle + \dots + |D-1\rangle$. Entanglement is created by the controlled Z -gates $Z_{\{ij\}}^\alpha = \sum_{g=0}^{d-1} (|g\rangle\langle g|)_i \otimes Z_j^{g\alpha}$, where $Z_q = \sum_{q=0}^{D-1} \omega^q |q\rangle\langle q|$ (with $\omega = e^{2\pi i/D}$) defines the

single-qudit Z -gate. For $\alpha = 1$ the structure reduces to non-weighted graph states, for $\alpha = \frac{1}{2}$ the weighted edges can be graphically represented by dashed lines.

As an example for a state which is MME but not GMME, consider the chain graph state of four ququarts:

$$|G^{(4)}\rangle = Z_{AB} Z_{BC} Z_{CD} |+\rangle^{\otimes 4}. \quad (14)$$

Encoding to eight qubits gives us the state (see Fig. 2, detailed calculations can be found in Appendix D [11]):

$$|G^{(2)}\rangle = Z_{A_1 B_1} Z_{B_1 C_1} Z_{C_1 D_1} Z_{A_2 B_2} Z_{B_2 C_2} Z_{C_2 D_2} \times Z_{A_2 B_1}^{\frac{1}{2}} Z_{B_1 C_2}^{\frac{1}{2}} Z_{C_2 D_1}^{\frac{1}{2}} |+\rangle^{\otimes 8}. \quad (15)$$

Now we apply two-qubit unitaries of the form $U_{ij} = |+\rangle\langle +|_i \otimes \mathbb{1}_j + |-\rangle\langle -|_i \otimes Z_j^{3/2}$ with $|\pm\rangle = (|0\rangle \pm |1\rangle)/\sqrt{2}$ on the two qubits of system A and D respectively and end up with

$$U_{A_1 A_2} U_{D_2 D_1} |G^{(2)}\rangle = Z_{B_1 C_2}^{\frac{1}{2}} |G_D^{(2)}\rangle, \quad \text{where} \quad (16)$$

$$|G_D^{(2)}\rangle = Z_{A_1 B_1} Z_{B_1 C_1} Z_{C_1 D_1} Z_{A_2 B_2} Z_{B_2 C_2} Z_{C_2 D_2} |+\rangle^{\otimes 8} \quad (17)$$

is a fully decomposable state with no diagonal edges.

Thus for the bipartitions $A|BCD$ or $D|ABC$ the state is decomposable and thereby not GMME. In fact, we find decomposability with respect to every possible bipartition (see Appendix D [11]). For claiming multilevel entanglement, we still have to exclude full decomposability, which is, as mentioned, a difficult task. We applied a numerical algorithm (Appendix E [11]) which strongly indicates non-decomposability with an maximal overlap of 0.8536 with the set of fully decomposable states.

Example 3. A genuine multilevel entangled state. — As a final example, consider the three ququart state

$$|\psi^{(4)}\rangle = \sum_{j=0}^3 |u_j\rangle |j\rangle |u_j\rangle - 2|3\rangle |3\rangle |3\rangle, \quad (18)$$

where $|u_0\rangle = |0\rangle + |1\rangle + |2\rangle + |3\rangle$, $|u_1\rangle = |0\rangle - |1\rangle + |2\rangle - |3\rangle$, $|u_2\rangle = |0\rangle + |1\rangle - |2\rangle - |3\rangle$, $|u_3\rangle = |0\rangle - |1\rangle - |2\rangle + |3\rangle$. This state corresponds to the six-qubit state $|\psi^{(2)}\rangle = Z_{123456} Z_{13} Z_{35} Z_{24} Z_{46} |+\rangle^{\otimes 2}$, a graph state with an additional hyperedge connecting all vertices [21]. For this state we found for all bipartitions the Schmidt coefficients to be $s_0 = 0.551$, $s_1 = s_2 = 0.5$, $s_3 = 0.443$ which leads to a non-zero determinant of $\det(S) = -0.0059$. Hence, $\text{rank}(S) \neq 1$ for all bipartitions and the state is non-decomposable for any bipartition. So the state is GMME, to be exact, genuine 3-partite 4-level entangled.

Conclusion. — We have introduced the notion of genuine multilevel entanglement. This formalizes the notion of high-dimensional entanglement that cannot be simulated directly with low-dimensional systems. We have provided methods to characterize those states for the

bipartite and multipartite case, including the construction of witnesses for an experimental test. The results can be interpreted as a cautionary tale with regards to naively employing standard entanglement characterization tools. Whereas under general local operations and classical communication, multiple copies of small dimensional systems are universal, this is not the case anymore in restricted scenarios, even having access to all possible local unitaries. This suggests that high-dimensional quantum systems do present a fundamentally different resource under realistic conditions.

For future research there are different topics to address. First, one may consider network scenarios, where a high-dimensional quantum state is distributed between several parties, and the correlations should be explained by low-dimensional states shared between subsets of the parties. Second, it would be desirable to develop a resource theory of high-dimensional entanglement, where not only the state preparation, but also the local operations (like filters) of the parties are considered. This may finally lead to a full understanding of quantum information processing with high-dimensional systems.

We thank Yu Cai, Wan Cong, and Valerio Scarani for discussions. This work has been supported by the ERC (Consolidator Grant 683107/TempoQ), the DFG, the Swiss National Science Foundation (Starting grant DIAQ and QSIT, and the Austrian Science Fund (FWF) through the START project Y879-N27 and the international project I3053-N27.

Appendix

A: Proof of Observation 1

Here we prove Observation 1, which states that a two ququart state is decomposable iff $\max \text{singval}(S) = 1$, where

$$S = \begin{bmatrix} s_0 & s_1 \\ s_2 & s_3 \end{bmatrix}. \quad (19)$$

First, let us consider two bipartite ququart states $|\psi\rangle$ and $|\varphi\rangle$. We prove that the maximal overlap between $|\psi\rangle$ and $|\varphi\rangle$, where each party is allowed to perform local unitary operations, is given by:

$$F_{max} = \max_{U_A, U_B} |\langle \psi | U_A \otimes U_B | \varphi \rangle| = \sum_{i=0}^{D-1} \eta_i \sigma_i \quad (20)$$

where $\eta_0 \geq \dots \geq \eta_3 \geq 0$ are the Schmidt coefficients of the state $|\psi\rangle$ and $\sigma_0 \geq \dots \geq \sigma_3 \geq 0$ are the Schmidt coefficients of the state $|\varphi\rangle$. This was already shown in Ref. [22], but we add this here for completeness. We start by writing the overlap in terms of coefficient matrices of the states $|\psi\rangle$ and $|\varphi\rangle$, that is we write $|\psi\rangle = \sum_{i,j} C_\psi^{ij} |ij\rangle$

as $C_\psi = \sum_{i,j} C_\psi^{ij} |i\rangle\langle j|$, and similarly for $|\varphi\rangle$. We have

$$\begin{aligned} F_{max} &= \max_{U_A, U_B} |\langle \psi | U_A \otimes U_B | \varphi \rangle| \\ &= \max_{U_A, U_B} |\text{tr}(C_\psi^\dagger U_A C_\varphi U_B^T)| \\ &= \sum_{i=0}^{D-1} s_i(C_\psi) s_i(C_\varphi). \end{aligned} \quad (21)$$

In the last step of Eq. (21) we used von Neumann's trace inequality:

$$|\text{tr}(\Lambda \Gamma)| \leq \sum_i \lambda_i \gamma_i \quad (22)$$

which holds for all complex $n \times n$ matrices Λ and Γ with ordered singular values $\lambda_i \leq \lambda_{i-1}$ and $\gamma_i \leq \gamma_{i-1}$. It was proven in Ref. [23] that equality in Eq. (22) can only be reached when Λ and Γ are simultaneously unitarily diagonalizable and hence both states need to have the same Schmidt basis. Therefore it is optimal to choose the encoding between the four-dimensional systems and the qubits in the Schmidt basis. Furthermore note that the singular values of the coefficient matrices are nothing but the Schmidt coefficients of the state. For the 2×2 matrix S the maximal singular value is given by

$$\alpha = \sqrt{\frac{1}{2}(1 + \sqrt{1 - 4 \det(S)^2})}. \quad (23)$$

Hence, we find that $\max \text{singval}(S) = 1$ iff $\det(S) = 0$, which finishes the proof of Observation 1. Other encodings lead to the same result since changing the encoding, can, for the special case of two qubits, be described by swapping rows or columns of S , which does not change its singular values. Note that for higher-dimensional systems (e.g., a qubit and a qutrit) the last point is not true, and this is the reason why we have to consider different matrices S there [see Eq. (8) in the main text].

B: Witnesses for the bipartite case

Here we show how to construct a witness operator for four-level entanglement. We are seeking for the state $|\xi\rangle$ which has the largest distance to the set of decomposable states and the smallest coefficient α such that the witness $\mathcal{W} = \alpha \mathbb{1} - |\psi\rangle\langle\psi|$ is positive on all decomposable states. Note that since \mathcal{D} is a convex set, it is sufficient to optimize over all pure decomposable states. In order to find $|\xi\rangle$ we compute

$$\begin{aligned} \alpha &= \min_S [\max \text{singval}(S)] \\ \text{s. t.: } &\det(S) \neq 0, \\ &s_0^2 + s_1^2 + s_2^2 + s_3^2 = 1, \\ &s_0 \geq s_1 \geq s_2 \geq s_3 \geq 0. \end{aligned} \quad (24)$$

First note that the maximal singular value of a 2×2 matrix is of the form of Eq. (23). In the following we separately analyse the cases $\det(S) < 0$ and $\det(S) > 0$.

For $\det(S) < 0$ we have to minimize $\det(S) = s_0 s_3 - s_1 s_2$. Since s_3 is by definition the smallest coefficient we choose $s_3 = 0$. Then we are left with $\max s_1 \cdot s_2$. For fixed s_0 we have that

$$s_1^2 + s_2^2 = \text{const.} \quad (25)$$

which is the equation of a circle. Therefore the problem is equivalent to maximizing the area of a rectangle with one corner at the origin and the other one on the circle defined by Eq. (25). The obvious solution is therefore $s_1 = s_2$. Since $s_0 \geq s_1$ the maximum is obtained at $s_0 = s_1 = s_2 = \frac{1}{\sqrt{3}}$.

For $\det(S) > 0$ we have to maximize $\det(S) = s_0 s_3 - s_1 s_2$. Therefore we have for any given s_0, s_3 to minimize $f(s_1) = s_1 \cdot s_2 = s_1 \sqrt{C - s_1^2}$ such that $s_0 \geq s_1 \geq s_2 \geq s_3 \geq 0$ and $C = 1 - s_0^2 - s_3^2$. The minimum of the function $f(s_1)$ is obtained at the boundary for $s_1 = s_3$, which implies $s_2 = s_3$. Therefore the maximum of the determinant is obtained at $s_1 = s_2 = s_3 = \frac{1}{2\sqrt{3}}$ and $s_0 = \sqrt{3/4}$.

We see that for dimension four the state with the largest distance to the set of decomposable states is the maximally entangled state of two qutrits. We observe that for increasing dimensions the distance between the maximally entangled states with lower dimension and the set of decomposable states decreases. Some analytical and numerical values are shown in Table I. This might lead to the conclusion that the multilevel entangled states get closer to the set of decomposable states for larger dimensions. However a proof that the maximally entangled states are the ones having the largest distance to the set of decomposable states is still missing.

C: Connection to the theory of Young tableaux

In this section we want to discuss the relation between the number of arrangements of Schmidt coefficients in the matrix S and the number of standard Young tableaux.

As mentioned in the main text, the complexity of characterizing the matrices S can be reduced, as we have to consider only those permutations which lead to different maximal singular values. First, note that given two probability distributions $\{p_i\}$ and $\{q_i\}$ the sum over the products $\sum_i \sqrt{p_i q_i}$ is maximal iff both are ordered in the same way. We can further assume in Eq. (4) in the main text that $\alpha_0 \geq \alpha_1$ and similarly for β_i , since exchanging the components of α and β correspond to exchanging rows or columns of S , which does not change its singular values. This implies that the entries of $|\alpha\rangle\langle\beta|$ decrease in each row and column. Different values for α_i and β_i thus lead to different arrangements. Consequently, we have

Source	rank	overlap
2×2 (4)	3	$\sqrt{\frac{1}{6}(3 + \sqrt{5})} \simeq 0.934$
2×3 (6)	5	$\sqrt{\frac{1}{10}(5 + \sqrt{17})} \simeq 0.955$
2×4 (8)	5	$\sqrt{\frac{1}{10}(5 + \sqrt{17})} \simeq 0.955$
	7	$\sqrt{\frac{1}{14}(7 + \sqrt{37})} \simeq 0.966$
3×3 (9)	5	$\sqrt{\frac{1}{10}(5 + \sqrt{17})} \simeq 0.955$
	7	$\sqrt{\frac{1}{14}(7 + \sqrt{33})} \simeq 0.954$
	8	$\sqrt{\frac{1}{16}(7 + \sqrt{48})} \simeq 0.965$
2×4 (10)	7	$\sqrt{\frac{1}{14}(7 + \sqrt{37})} \simeq 0.966$
	9	$\sqrt{\frac{1}{18}(9 + \sqrt{65})} \simeq 0.973$
2×6 (12)	7	$\sqrt{\frac{1}{14}(7 + \sqrt{37})} \simeq 0.966$
	9	$\sqrt{\frac{1}{18}(9 + \sqrt{65})} \simeq 0.973$
7×7 (49)	11	$\sqrt{\frac{1}{22}(11 + \sqrt{101})} \simeq 0.9781$

Table I: This table shows the analytical and numerical fidelities of the maximally entangled state $|\psi\rangle = 1/\sqrt{D} \sum_{i=0}^{D-1} |ii\rangle$ with all decomposable states for a given dimension of the source.

to optimize S under the constraints that the entries of S must be non-increasing in each row from left to right and in each column from top to bottom.

To see the connection to Young tableaux, let us first recall the definition of a Young diagram. Given some number $N \in \mathbb{N}$ we call $\lambda = (\lambda_1, \lambda_2, \dots, \lambda_n)$ a partitioning of the number N , that is $\sum_k \lambda_k = N$, $\lambda_1 \geq \lambda_2 \geq \dots \geq \lambda_n$, and $\lambda_i \in \mathbb{N}$. Then a Young diagram is an arrangement of left-justified rows, where the number of boxes in the k -th row is given by λ_k (see Fig. 3).

A Young tableau of shape λ is a filling of the numbers $1, 2, \dots, n$ into the boxes of the Young diagram such that every number appears exactly once. A Young tableau is called standard if the numbers are increasing in each row and each column. From here it is straightforward to see that this problem is equivalent to the problem of finding the number of possible arrangements of the Schmidt coefficients in the matrix S under the constraints that we discussed above. The number of possible arrangements that could lead to different maximal singular values is simply given by the number of standard Young tableaux consisting of $d_1 \times d_2$ boxes, arranged in a single block. This number is given by the so-called hook-length formula [14]

$$\mathcal{N} = \frac{n!}{\prod_{(i,j)} h_{i,j}}, \quad (26)$$

where $h_{i,j}$ is called a hook-length of the box (i, j) . For a given box (i', j') , its hook consists of all boxes with either $(i = i', j > j')$ or $(i > i', j = j')$ and the box itself. The length of the hook is then given by the number of boxes in the hook. For a Young tableau of $d_1 \times d_2$ boxes this

$$N = 8 \quad \lambda = (4, 3, 1)$$

1	2	6	7
3	5	8	
4			

Figure 3: This figure shows an example of a standard Young tableau for $N = 8$ and a partitioning $\lambda = (4, 3, 1)$. The numbers $1, \dots, 8$ are arranged in such a way that their values increase in each row and each column.

simplifies to

$$\mathcal{N} = \frac{(d_1 \times d_2)!}{\prod_{i=1}^{d_1} \prod_{j=1}^{d_2} (i + j - 1)}. \quad (27)$$

In case one is only interested whether or not a state is decomposable, the number of different matrices that lead to a maximal singular value of one can be further reduced. This is due to the additional constraint that if the matrix S has rank one all the rows as well as the columns must be mutually linearly dependent. Then, it is easy to see that the following algorithm can solve the problem. We start again by filling the Schmidt coefficients in an array such that their values are non-increasing in each row and each column. We can fix the upper left entry to be the largest element. Whenever we get in a situation in which we fix the constant between two rows or columns we check whether there are some remaining Schmidt coefficients which lead to linearly dependent rows or columns. If this is the case, we fill the array with the appropriate number and continue. If these numbers do not exist, we abort and have to start all over again with a different arrangement. It is obvious that if there exists an arrangement which leads to a matrix with rank one, then the algorithm will find it. Using the formalism of Young tableaux we can again calculate the maximum number of different matrices that we need to check. First note that when we apply the algorithm we always fix the values of the entries in the first row and the first column. The only thing that changes is the order in which we fill the entries. The number of all possible ways to do this is again given by a number of standard Young tableaux consisting of a single row and a single column. By applying the hook length formula we obtain

$$\begin{aligned} \mathcal{N}' &= \frac{(d_1 + d_2 - 1)!}{(d_1 + d_2 - 1) \times (d_1 - 1)! \times (d_2 - 1)!} \\ &= \frac{(d_1 + d_2 - 2)!}{(d_1 - 1)! \times (d_2 - 1)!}. \end{aligned} \quad (28)$$

D: Examples

In this section, we provide some notes on Example 1 (fully decomposable state) as well as a detailed proof for

Example 2 (MME state) for the multipartite exemplary states given in the main text. Furthermore we present another interesting fully decomposable state of six qubits.

Example 1. GHZ States

LU-equivalence of GHZ- and star-type graph states. Here we show the equivalence of star-type graph states and GHZ states in arbitrary dimension and system size under local unitary (LU) operations. Decomposability is a property of a state which does not change under LU-operations on the original state, therefore it is sufficient to show that $|G_{star}\rangle \stackrel{LU}{\equiv} |GHZ^{(D)}\rangle$ for any dimension D and any number of qudits N .

Star-type graphs are graphs where one central vertex is connected to any other vertex by an edge, and no other edges are present. For the corresponding quantum state we have according to Eq. (13) in the main text $|G_{star}\rangle = \prod_{q=2}^N Z_{1q}|+\rangle^{\otimes N}$. This can be simplified to:

$$\begin{aligned} |G_{star}\rangle &= \sum_{p=0}^{N-1} |p\rangle_1 \bigotimes_{q=2}^N |+_p\rangle_q \\ &\propto |0\rangle_1 |+_0\rangle_2 \dots |+_0\rangle_N + |1\rangle_1 |+_1\rangle_2 \dots |+_1\rangle_N \\ &\quad + \dots + |D-1\rangle_1 |_{+D-1}\rangle_2 \dots |_{+D-1}\rangle_N. \end{aligned} \quad (29)$$

Here we use the (D -dimensional) single qudit states $|+_i\rangle = \frac{1}{\sqrt{D}} \sum_{k=0}^{D-1} \omega^{ki} |k\rangle$ with $\omega = e^{2\pi i/D}$, note that $|+_0\rangle = |+_D\rangle$ in our previous notation. Since $\langle +_i | +_j \rangle = \delta_{ij}$ the set $\{|+_i\rangle\}$ forms a basis of \mathbb{C}^D . Eq. (29) is, up to local rotations on all subsystems except the first, equal to $|GHZ^{(D)}\rangle$.

Full decomposability of a $6 \times 6 \times 6$ system To clarify the proof of Eq. (12) in the main text, we exemplarily do the complete calculation for a system of three parties each of which has dimension six, such that the prime decomposition $D = 2 \times 3$ equals access to a qubit and a qutrit. The state, up to normalization, reads $|GHZ^{(6)}\rangle = \sum_{\ell=0}^5 |\ell\ell\ell\rangle$. The encoding and resorting of the order, which groups the subsystems of the qubits and qutrits respectively, then gives the six-partite state:

$$\begin{aligned} |GHZ^{(6)}\rangle &\stackrel{enc.}{=} |000000\rangle + |010101\rangle + |020202\rangle \\ &\quad + |101010\rangle + |111111\rangle + |121212\rangle \\ &\stackrel{res.}{=} |000000\rangle + |000111\rangle + |000222\rangle \\ &\quad + |111000\rangle + |111111\rangle + |111222\rangle \\ &= (|000\rangle + |111\rangle) \otimes (|000\rangle + |111\rangle + |222\rangle) \end{aligned} \quad (30)$$

which shows decomposability into $|GHZ^{(2)}\rangle$ and $|GHZ^{(3)}\rangle$. The generalization to an arbitrary number of systems N and arbitrary dimension D follows straightforward.

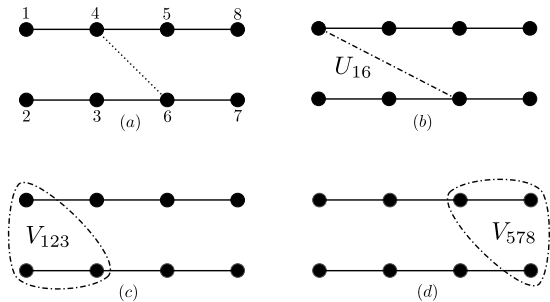


Figure 4: Example of a state that is MME but not genuine MME. The four-ququart chain-type graph is encoded into LU-equivalent eight-qubit states. (a): The equivalence to this state has already been shown in the main text, see Fig. 2. (b): The state is also equivalent to this configuration, see Eq. (37). (c) and (d): These equivalences follow from Eq. (35). In summary, the state is decomposable with respect to all possible bipartitions.

Example 2: Graph states

Here we present the calculation for the four-ququart graph states, see also Fig. 4 and Fig. 2 in the main text. To start, the chain graph state of $N = 4$ ququarts is given by

$$\begin{aligned} |G^{(4)}\rangle &= \tilde{Z}_{AB}\tilde{Z}_{BC}\tilde{Z}_{CD}|+\rangle^{\otimes 4} \\ &= \sum_{ABCD=0}^3 \omega_{(4)}^{AB}\omega_{(4)}^{BC}\omega_{(4)}^{CD}|ABCD\rangle. \end{aligned} \quad (31)$$

Here $\tilde{Z}_{ij} = \text{diag}(1, i, -1, -i)$ is the ququart controlled Z-gate and $\omega_{(4)} = e^{2\pi i/4} = i$. We use the computational basis $|ABCD\rangle$ to simplify the encoding process. The ququarts corresponding to (A, B, C, D) are decomposed into two qubits each with the labels $(A_1, A_2, B_1, B_2, C_1, C_2, D_1, D_2) = (1, 2, 4, 3, 5, 6, 8, 7)$, see Fig. 4(a).

To represent the ququart state, we make the replacements: $A \rightarrow 2A_1 + A_2$, $B \rightarrow 2B_2 + B_1$, $C \rightarrow 2C_1 + C_2$ and $D \rightarrow 2D_2 + D_1$, as this reproduces for an additional replacement of the $\sum_{A,B,C,D=0}^3 \rightarrow \sum_{A_1 \dots D_2=0}^1$ the same exponents as in Eq. (31). Then we have:

$$\begin{aligned} |G^{(4)}\rangle &\stackrel{enc.}{=} |G^{(2)}\rangle \\ &= \sum_{A_1 \dots D_2=0}^1 \omega_{(4)}^{(2A_1+A_2)(2B_2+B_1)} \omega_{(4)}^{(2B_2+B_1)(2C_1+C_2)} \\ &\quad \omega_{(4)}^{(2C_1+C_2)(2D_2+D_1)} |A_1 A_2 B_1 B_2 C_1 C_2 D_1 D_2\rangle. \end{aligned} \quad (32)$$

We furthermore use $\omega_{(4)} = e^{\frac{i\pi}{2}} = \omega_{(2)}^{\frac{1}{2}}$ and $\omega_{(2)}^{2c} = 1$, $c \in$

\mathbb{N} and can simplify Eq. (32)

$$\begin{aligned} |G^{(2)}\rangle &= \sum_{A_1 \dots D_2=0}^2 \omega_{(2)}^{A_1 B_1} \omega_{(2)}^{A_2 B_2} \omega_{(2)}^{B_2 C_2} \omega_{(2)}^{B_1 C_1} \omega_{(2)}^{C_1 D_1} \omega_{(2)}^{C_2 D_2} \\ &\quad \omega_{(2)}^{\frac{A_2 B_1}{2}} \omega_{(2)}^{\frac{B_1 C_2}{2}} \omega_{(2)}^{\frac{C_2 D_1}{2}} |A_1 A_2 B_1 B_2 C_1 C_2 D_1 D_2\rangle \\ &= Z_{A_1 B_1} Z_{A_2 B_2} Z_{B_2 C_2} Z_{B_1 C_1} Z_{C_1 D_1} Z_{C_2 D_2} \\ &\quad Z_{A_2 B_1}^{\frac{1}{2}} Z_{B_1 C_2}^{\frac{1}{2}} Z_{C_2 D_1}^{\frac{1}{2}} |+\rangle^{\otimes 8}. \end{aligned} \quad (33)$$

Here, $Z_{ij} = \text{diag}(1, -1)$ is the qubit-controlled Z-gate, this state is shown in left side of Fig. 2 in the main text. We then apply $V_{A_1 A_2}$, $V_{B_1 B_2}^{\frac{3}{2}}$ and $V_{D_1 D_2}^{\frac{3}{2}}$ to $|G^{(2)}\rangle$. Those are for the further analysis in this example defined as

$$V_{X_1 X_2} = (|+\rangle\langle +|)_{X_1} \otimes \mathbb{1}_{X_2} + (|-\rangle\langle -|)_{X_1} \otimes Z_{X_2}, \quad (34)$$

where for $X = A, B, C, D$ all $V_{X_1 X_2}$ are included in the set of vertical unitaries $\{U_{\text{Vert}}\}$. By straightforward calculation, one verifies:

$$\begin{aligned} (V_{A_1 A_2} V_{B_1 B_2}^{\frac{3}{2}} V_{D_1 D_2}^{\frac{3}{2}}) |G^{(2)}\rangle &= V_{A_1 A_2 B_2} |G_{\mathcal{D}}^{(2)}\rangle, \\ (V_{D_1 D_2} V_{C_1 C_2}^{\frac{3}{2}} V_{A_1 A_2}^{\frac{3}{2}}) |G^{(2)}\rangle &= V_{C_1 D_1 D_2} |G_{\mathcal{D}}^{(2)}\rangle. \end{aligned} \quad (35)$$

This means that for the question of decomposability the weighted diagonal edges have the same effect on the decomposable state $|G_{\mathcal{D}}^{(2)}\rangle$ as one hyper-edge connecting three qubits either one or the other end of the chain, see Fig. 4(c) and Fig. 4(d). The mentioned hyper-edge is formally a three-qubit unitary of the form

$$V_{X_1 X_2 Y_1} = (|+\rangle\langle +|)_{X_1} \otimes \mathbb{1}_{X_2 Y_1} + (|-\rangle\langle -|)_{X_1} \otimes V_{X_2 Y_1} \quad (36)$$

with $V_{X_2 Y_1}$ as defined in Eq. (34) and $|G_{\mathcal{D}}^{(2)}\rangle$ is a decomposable state, defined in Eq. (17) in the main text.

Furthermore, one can directly check that we can replace the three weighted Z-gates ($Z_{ij}^{\frac{1}{2}}$) in Eq. (33) by one weighted edge acting on qubits A_1 and C_2

$$|G^{(2)}\rangle = U_{A_1 A_2}^{\frac{3}{2}} U_{B_1 B_2}^{\frac{3}{2}} U_{A_1 C_2} |G_{\mathcal{D}}^{(2)}\rangle \quad (37)$$

with $U_{A_1 C_2} = (|+\rangle\langle +|)_{A_1} \otimes \mathbb{1}_{C_2} + (|-\rangle\langle -|)_{A_1} \otimes Z_{C_2}$ and two vertical unitaries $U_{A_1 A_2}^{\frac{3}{2}}$ and $U_{B_1 B_2}^{\frac{3}{2}}$ [see Fig. 4(b)].

From Eq. (35) and Eq. (37) we see that whereas this state is not decomposable, there exists for every bipartition a representation of this state, for which the S -matrix has rank 1. In Fig. 4, the different equivalent representations of the state are shown graphically. Each option presents decomposability with respect to another bipartite split, such that all possible ones are covered. However, to exclude genuine MME, let us once again stress that the existence of one split exhibiting decomposability is enough.

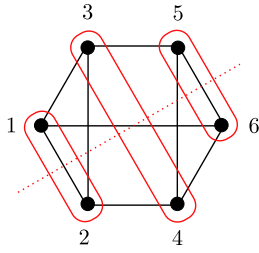


Figure 5: The maximally entangled state on six qubits represents a decomposable three ququart state.

The maximally entangled state of six qubits

We have already seen that the highly entangled GHZ states are not necessarily multilevel entangled. Therefore one might ask the following question: Are there other highly entangled states which are not multilevel entangled? One example is the three-ququart state that corresponds to the absolutely maximally entangled state of six qubits (see Fig. 5). The six-qubit state is given by

$$|G^{(2)}\rangle = Z_{12}Z_{34}Z_{56}Z_{23}Z_{36}Z_{45}Z_{24}Z_{35}Z_{16}|+\rangle^{\otimes 6} \quad (38)$$

and corresponds to a graph state. Nevertheless, this state is fully decomposable. To prove this, we first mention that via local complementation [20] (LC), we can obtain:

$$|G^{(2)}\rangle \xrightarrow[\text{on } 1,2,5,3]{\text{LC}} Z_{12}Z_{56}Z_{14}Z_{23}Z_{36}Z_{45}Z_{15}Z_{26}|+\rangle^{\otimes 6} \quad (39)$$

Comparing Eq. (38) and Eq. (39), the difference between those is depicted in Fig. 5 on the right side. Whereas the first contains diagonal connections (which contradicts a direct decomposition), the second form shows that these can be replaced by vertical and horizontal ones. Therefore we can reach the original state by starting from a decomposable state.

E: Algorithm for testing full decomposability

In this section we explain the algorithm that we used to test whether or not the four ququart chain-graph state $|\psi\rangle$ in Eq. 14 in the main text. The aim is to test whether or not the state $|\psi\rangle$ can be written as $|\psi\rangle \stackrel{?}{=} U_A \otimes U_B \otimes U_C \otimes U_D |Q\rangle \otimes |R\rangle$, see also Fig. 6. Thus, we want to compute

$$\max_{\substack{U_A \dots U_D \\ |Q\rangle |R\rangle}} |\langle Q | \langle R | U_A \otimes U_B \otimes U_C \otimes U_D |\psi\rangle|. \quad (40)$$

The idea is to choose initial states $|Q\rangle$ and $|R\rangle$, as well as unitaries U_A, \dots, U_D at random and then optimize

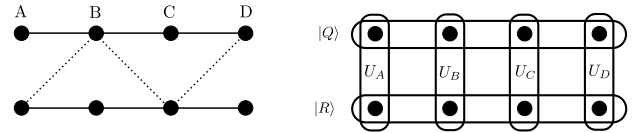
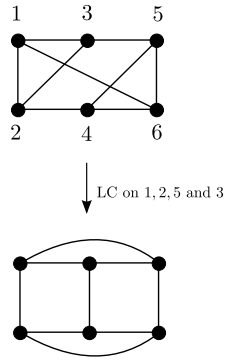


Figure 6: We ask whether the state on the left can be constructed by first preparing states $|Q\rangle$ and $|R\rangle$ and then applying local unitary operations U_A, \dots, U_D . Since this is not possible the state is not decomposable, it is MME.

the states and unitaries iteratively, until a fix-point is reached. The point is that any of the iteration steps can be performed analytically. In order to optimize the state $|Q\rangle$, we fix the unitaries U_A, \dots, U_D and the state $|R\rangle$. We obtain the optimal choice of $|Q\rangle$ by computing $\max_Q |\langle Q | \langle R | U_A \otimes U_B \otimes U_C \otimes U_D |\psi\rangle| = \max_Q |\langle Q | \tilde{\psi}\rangle|$. We have that $|Q\rangle \propto |\tilde{\psi}\rangle$ is optimal up to normalization. The similar argument holds for $|R\rangle$. For optimizing the local unitaries we fix any unitary but the one we want to optimize, say U_A . Then, we have

$$\begin{aligned} & \max_{U_A} |\langle Q | \langle R | U_A \otimes U_B \otimes U_C \otimes U_D |\psi\rangle| \\ &= \max_{U_A} |\langle Q | \langle R | U_A |\tilde{\psi}\rangle| \\ &= \max_{U_A} |\text{tr}(U_A |\tilde{\psi}\rangle \langle Q | \langle R|)| \\ &= \max_{U_A} |\text{tr}_A(U_A \varrho_A)| = \sum_i s_i(\varrho_A) \end{aligned} \quad (41)$$

where $\varrho_A = \text{tr}_{BCD}(|\tilde{\psi}\rangle \langle Q | \langle R|)$. We write ϱ_A in the singular value decomposition and we get $\varrho_A = U D V^\dagger$. Then we choose $U_A = V U^\dagger$ and hence

$$|\text{tr}_A(U_A \varrho_A)| = |\text{tr}(D)| = \sum_i s_i(\varrho_A). \quad (42)$$

* These two authors contributed equally.

- [1] M. Krenn, M. Huber, R. Fickler, R. Lapkiewicz, and A. Zeilinger, Proc. Natl. Acad. Sci. USA **111**, 6243 (2014).
- [2] G. A. Howland, S. H. Knarr, J. Schneeloch, D. J. Lum, and J. C. Howell, Phys. Rev. X **6**, 021018 (2016).
- [3] A. Martin, T. Guerreiro, A. Tiranov, S. Designolle, F. Fröwis, N. Brunner, M. Huber, and N. Gisin, Phys. Rev. Lett. **118**, 110501 (2017).
- [4] H. Bechmann-Pasquinucci and W. Tittel, Phys. Rev. A **61**, 062308 (2000).
- [5] N. J. Cerf, M. Bourennane, A. Karlsson, and N. Gisin, Phys. Rev. Lett. **88**, 127902 (2002).
- [6] A. Sanpera, D. Bruß, and M. Lewenstein, Phys. Rev. A **63**, 050301 (2001).
- [7] G. Sentís, C. Eltschka, O. Gühne, M. Huber, and J. Siewert, Phys. Rev. Lett. **117**, 190502 (2016).
- [8] N. Brunner, S. Pironio, A. Acín, N. Gisin, A. Allan Methot, and V. Scarani, Phys. Rev. Lett. **100**, 210503 (2008).

- [9] Y. Cai, Quantum sizes: Complexity, Dimension and Many-box Locality, PhD thesis, Singapore (2015).
- [10] W. Cong, Y. Cai, J.-D. Bancal, and V. Scarani, *Phys. Rev. Lett.* **119**, 080401 (2017).
- [11] The Appendices can be found in the supplemental material.
- [12] B. M. Terhal, *Phys. Lett. A* **271**, 319 (2000).
- [13] O. Gühne and G. Tóth, *Phys. Reports* **474**, 1 (2009).
- [14] H. Georgi, “Lie Algebras In Particle Physics”, *Westview Press*, 2nd ed. (1999).
- [15] S. Jevtic, D. Jennings, and T. Rudolph, *Phys. Rev. Lett.* **108**, 110403 (2012).
- [16] A. Peres, *Phys. Lett. A* **202**, 16 (1995).
- [17] M. Huber and R. Sengupta, *Phys. Rev. Lett.* **113**, 100501 (2014).
- [18] C.-M. Li, K. Chen, A. Reingruber, Y.-N. Chen, and J.-W. Pan, *Phys. Rev. Lett.* **105**, 210504 (2010).
- [19] A. Keet, B. Fortescue, D. Markham, and B. C. Sanders, *Phys. Rev. A* **82**, 062315 (2010).
- [20] M. Hein, W. Dür, J. Eisert, R. Raussendorf, M. Van den Nest, and H.-J. Briegel, [quant-ph/0602096](https://arxiv.org/abs/quant-ph/0602096).
- [21] M. Rossi, M. Huber, D. Bruß, and C. Macchiavello, *New J. Phys.* **15**, 113022 (2013).
- [22] O. Gühne, and N. Lütkenhaus, *Phys. Rev. Lett.* **96**, 170502 (2006).
- [23] L. Mirsky, *Monatshefte für Mathematik* **79**, 303 (1975).